QUANTUM MEASUREMENTS WITH POST-SELECTION

IISER PUNE

A thesis submitted towards partial fulfilment of
BS-MS Dual Degree Programme

by

ANIRBAN CH NARAYAN CHOWDHURY

under the guidance of

PRASANTA K. PANIGRAHI

DEPARTMENT OF PHYSICAL SCIENCES
IISER KOLKATA

INDIAN INSTITUTE OF SCIENCE EDUCATION AND
RESEARCH PUNE

Certificate

This is to certify that this thesis entitled "Quantum Measurements with Post-selection" submitted towards the partial fulfilment of the BS-MS dual degree programme at the Indian Institute of Science Education and Research Pune represents original research carried out by Anirban Ch Narayan Chowdhury at the Indian Institute of Science Education and Research Kolkata, under the supervision of Prasanta K. Panigrahi during the academic year 2012-2013.

Student

ANIRBAN CH NARAYAN CHOWDHURY

Supervisor

PRASANTA K. PANIGRAHI

Acknowledgements

Abstract

A quantum measurement with post-selection defines measurement outcomes consistent with given initial and final states of the system being measured, through a change recorded on a measuring device or pointer. As the initial and final states of the system, known as *pre-selection* and *post-selection* respectively, need not be eigenstates of the measurement operator, post-selected measurement can consistently give rise to non-eigenvalue measurement outcomes, particularly if the initial pointer state has a large associated uncertainty. In the limit of a very weak interaction between the system and the device, the measurement outcome is the weak value, which can be larger than any known eigenvalue and can even be complex. Even though their physical meaning is debated, weak values show patterns consistent with classical logic and have been used to address conceptual problems in quantum mechanics. Weak measurements have found immense use in experimental techniques to amplify and detect small signals, and for precision measurements. In this thesis, we review the theory of post-selected measurements and consequently that of weak measurements. We demonstrate the possibility of achieving higher signal-to-noise ratio of amplification using simplified Hermite Gauss and Laguerre Gauss modes instead of Gaussian wavefunction as pointer. We also explore the upper limit of amplification by calculating exact expressions of pointer shifts. Finally, we propose a method of reconstructing the state of a spin-$\frac{1}{2}$ particle using post-selected quantum measurements.

Contents

Chapter 1

Introduction

Measurement occupies a special place in quantum mechanics. In classical physics, a measuring process is subject to the usual laws that govern all physical processes. For example, consider a free particle moving in an electric field. Its motion is according to the laws of classical mechanics and electromagnetism. Now, if we measure its position by flashing light on it, the process might introduce some change in its motion, but the change would be as per the same laws. In quantum mechanics, however, this does not happen. The "motion", or rather the evolution of the particle's wavefunction, is governed by the Schrödinger's equation. But a description of the measurement of its position requires a postulate of *wavefunction collapse*. This is because quantum mechanics allows the particle to be in a superposition of multiple possible states of position but a measurement invariably locates the particle at one particular location.

Mathematically, a quantum mechanical system is described by a vector in Hilbert space, denoted by the ket $|\psi\rangle$ in the Dirac notation. The evolution of the system can be described by the action of unitary matrices on this state vector, $|\psi\rangle \rightarrow \hat{U}|\psi\rangle$. But unitary matrices are insufficient to describe a measurement on $|\psi\rangle$. In quantum theory, any measurable property has a corresponding Hermitian operator, whose eigenvalues correspond to the possible measurement outcomes. In general, $|\psi\rangle$ can be some combination of the eigenvectors of an observable $\hat{A}$, i.e.,

$$|\psi\rangle = \sum_i c_i |a_i\rangle \tag{1.1}$$

where $\hat{A}|a_i\rangle = a_i|a_i\rangle$. Measurement of $\hat{A}$ will give an outcome a_i with probability $|\langle a_i|\psi\rangle|^2$ as calculated from the Born rule, in the process changing the state to the corresponding eigenvector $|a_i\rangle$. The problem is that

the projection of $|\psi\rangle$ to $|a_i\rangle$ is non-unitary. Following a model given by von Neumann, the system and the measuring device can be thought of as interacting quantum systems, together undergoing a unitary evolution. However, if the system being measured is initially in a superposition state, at the end of the evolution a projection is required to yield definite measurement outcomes. The quantum interaction between the two fails to capture the dynamics of collapse.

As a quantum measurement is probabilistic, specifying an initial state of a system is generally not sufficient to predict the outcome of any measurement performed on it. Based on this consideration, Aharonov *et al.* introduced the concept of a *post-selected measurement* where, in addition to an initial state $|\chi_i\rangle$, a final state $|\chi_f\rangle$ of the system is also specified [1]. Generally, $|\chi_f\rangle$ need not be an eigenstate of the observable $\hat{A}$ being measured, and the post-selection would therefore disturb whatever state of $\hat{A}$ the system was it. Therefore, Aharonov, Albert and Vaidman devised the notion of a *weak measurement* [2] - involving a von Neumann type measurement interaction with a very small coupling strength - that would minimally disturb the state being measured. The measurement interaction is followed by a post-selection, only after which the measuring device was observed. In the von Neumann model, the measurement outcomes are determined from the shifts in a pointer observable of the measuring device.

It was found that for such a weak measurement, the pointer shifts can be arbitrarily large, implying that the measurement outcomes, or *weak values*, defined in this manner can be many times larger than the eigenvalues of the measurement operator. In the most general case, weak values of an operator are different from its eigenvalues, which has led many to question the validity of labelling these weak values as measurement outcomes [3][4]. The proponents of weak measurements, however, insist that weak values are physically meaningful quantities, characterizing the system between its initial and final states [5][1]. The question of whether post-selection can produce errors in normal measurement procedures has also been addressed [6]. These strange weak values have also been observed experimentally [7][8]. Well-known conceptual paradoxes in quantum mechanics have been revisited and analysed in the context of weak values [9], and weak measurement based versions of these have been experimentally implemented [10].

Notwithstanding the conceptual issues surrounding them, weak measurements have found considerable practical applications. It has emerged as

a powerful technique for amplifying and detecting small signals [11][12]. Weak values have also been used to calculate average trajectories of photons [13], as well as to compute tunnelling times [14][15]. In addition, they have provided new methods of reconstructing quantum wavefunctions [16] and quantum state tomography [17]. The connection between sub-Planck structures in phase-space and weak measurements have also been explored in the context of quantum cat states [18].

In this thesis, we review weak measurements as a special case of more general measurements with post-selection and study a few applications. The second chapter introduces the basic theory, starting with the von Neumann measurement model and then adding post-selection, in the process re-deriving the weak measurement condition. The third chapter studies weak-value amplification for different pointer states, where we show that the amplification can be enhanced by using non-Gaussian pointer states. We also estimate the amplification limits through exact calculations. In the final chapter we show that post-selection can be a useful tool to reconstruct and extract information from quantum states. Throughout this thesis, we have used units where $\hbar = 1$.

Chapter 2

Quantum Measurements: Projective, Post-selected and Weak

The aim of this chapter is to introduce the concept of post-selected and weak measurements. For this purpose, we begin with the von Neumann model of projective measurements. Post-selection is introduced in the context of this model, and weak measurement is later shown to be a special case of post-selected measurements. The actual physical phenomenon taking place is clarified using the example of a spin-$\frac{1}{2}$ particle. Subsequently we discuss the physical implications of such measurements and their experimental implementations. The chapter ends with general methods of deriving the necessary expressions, both approximate and exact.

2.1   The von Neumann measurement model

A commonly used model of quantum measurement was given by John von Neumann [19], which we shall be using extensively in this thesis. Here, we outline this model following the treatment of Aharonov and Rohrlich [20]. In this model, the measuring process is devised as a quantum interaction between a "system" S and a "measuring device" D. The aim is to measure some observable $\hat{A}$ of S, as recorded by an observable $\hat{Q}$ of D. The interaction should be such that it produces a change in $\hat{Q}$ that corresponds to the value of $\hat{A}$, and in the process, the value of the observable should not change. The simplest interaction Hamiltonian that can be

written down following these criteria is

$$\hat{H}_{int} = g(t)\hat{A} \otimes \hat{P} \tag{2.1}$$

where $[\hat{Q}, \hat{P}] = i$, and $g(t)$ is essentially the strength of the interaction. The measurement interaction is assumed to take place for a finite time interval t_0, i.e., $g(t)$ is non-zero only for $0 \leq t \leq t_0$. The change in $\hat{Q}$ due to this interaction can be determined from the Heisenberg equation of motion,

$$\frac{d\hat{Q}}{dt} = i[\hat{H}, \hat{Q}] \tag{2.2}$$

where $\hat{H}$ also includes the individual Hamiltonians of S and D, $\hat{H}_s$ and $\hat{H}_d$ respectively.

$$\hat{H} = \hat{H}_s + \hat{H}_d + \hat{H}_{int} \tag{2.3}$$

The total change in $\hat{Q}$ after the interaction is therefore,

$$\begin{aligned}
\Delta\hat{Q}_d &= i \int_0^{t_0} dt[\hat{H}, \hat{Q}] \\
&= i \int_0^{t_0} dt[\hat{H}_d + \hat{H}_s + g(t)\hat{A} \otimes \hat{P}, \hat{Q}] \\
&= i \int_0^{t_0} dt[\hat{H}_d, \hat{Q}] + g\hat{A}
\end{aligned} \tag{2.4}$$

If we now further assume that the interaction occurs for a vanishingly small time, i.e., $t_0 \to 0$, only $g\hat{A}$ survives in the above expression.

Now, how do we perform a measurement of $\hat{A}$ with such an interaction? First, we initialize our device or pointer as $|q\rangle$, an eigenstate of $\hat{Q}$. If our system's state is an eigenstate of $\hat{A}$, i.e., $\hat{A}|a_i\rangle = a_i|a_i\rangle$, the combined system $S + D$ evolves as

$$|a_i\rangle \otimes |q\rangle \to |a_i\rangle \otimes |q + ga_i\rangle$$

The change in the meter observable $\hat{Q}$ is thus $\delta q = ga_i$. As the interaction strength g is previously known, a_i can be calculated from the meter shift. If the initial state is a superposition, e.g., $|\psi\rangle = 1/\sqrt{2}\,(|a_1\rangle + |a_2\rangle)$, the final state of the combined system is

$$|\Phi\rangle = \frac{1}{\sqrt{2}}\left(|a_1\rangle|q + ga_1\rangle + |a_2\rangle|q + ga_2\rangle\right) \tag{2.5}$$

This is an entangled state, and a one-to-one correspondence has been achieved with an eigenstate of $\hat{A}$ and that of $\hat{Q}$. Each possible measurement outcome

of $\hat{A}$ is correlated to a unique shift in q. But the final is still a superposition. To measure the shift in our meter, we still have to perform a projection to the eigenbasis of $\hat{Q}$. Such a projection is an additional imposition, not captured by the unitary interaction between S and D.

The answer to the question why and how collapse of the state vector occurs is not the subject of this thesis. For the moment, we note that this is still considered an open problem. It has been shown by Zurek and others that decoherence due to interaction with the environment leads to eventual loss of superposition, or coherence. Decoherence cannot, however, predict which particular outcome will arise in a particular measurement.

2.2 Measurements with post-selection

The idea of measurement with a post-selection was introduced by Aharonov *et al.* in 1988 in the context of weak measurements [2]. However, post-selection can be implemented without resorting to the conditions that weak measurements require. We therefore introduce post-selection prior to a discussion of weak measurements.

The idea of post-selection is as follows:
we perform a measurement on a quantum system, conditioned to the fact that the system is later detected, i.e., *post-selected* in a particular state. Given an initial quantum state $|\chi_{\text{in}}\rangle$, a measurement of $\hat{A}$ with post-selection $|\chi_{\text{fi}}\rangle$ implies that we record the outcome of the measurement only if the system is found in the state $|\chi_{\text{fi}}\rangle$ after the measurement. Usually, we shall be dealing with measurements on an ensemble of identically prepared systems. In the classical case, a post-selection would then be equivalent to choosing a particular sub-ensemble. For quantum systems however, post-selection is generally more complicated. The initial preparation step is often referred to as the *pre-selection* step and an ensemble of systems, identically pre- and post-selected in this manner is called a pre- and post-selected ensemble (PPS).

There are two possible scenarios for measurements with post-selection in the quantum case. Firstly, a post-selection can be performed after the meter is observed, i.e,, after a state vector collapse. In this case, the measurement outcomes are the eigenvalues of $\hat{A}$; the probability of an outcome a_j (i.e., a shift of ga_j in the pointer) is given by

$$P(a_j) = \left(\frac{|\langle \chi_{\text{in}}|a_j\rangle||\langle a_j|\chi_{\text{fi}}\rangle|}{|\langle \chi_{\text{in}}|\chi_{\text{fi}}\rangle|} \right)^2 \tag{2.6}$$

whereas without post-selection it would have been $|\langle a_j|\chi_{\text{in}}\rangle|^2$.

In the other case, the measurement interaction $\hat{U}_{int}$ precedes the post-selection, but the projection on the measuring device is performed *after* post-selection. Then, the final state of a measuring device previously initialized in the state $|\psi_{\text{in}}\rangle$, is

$$|\psi_{\text{fi}}\rangle = \frac{\langle\chi_{\text{fi}}|\hat{U}_{int}|\chi_{\text{in}}\rangle|\psi_{\text{in}}\rangle}{\left|\langle\chi_{\text{fi}}|\hat{U}_{int}|\chi_{\text{in}}\rangle|\psi_{\text{in}}\rangle\right|} \tag{2.7}$$

If the measurement interaction is of the von Neumann type and $|\psi_{\text{in}}\rangle = |q\rangle$, we can write

$$|\psi_{\text{fi}}\rangle = \frac{1}{N}\sum_j \langle a_j|\chi_{\text{in}}\rangle\langle\chi_{\text{fi}}|a_j\rangle|q + ga_j\rangle \tag{2.8}$$

where N is the normalization.

If we now perform a projection of $\hat{Q}$, we get a distribution of discrete shifts, $ga_1, ga_2, ...$etc, as before. The probability of obtaining the shift ga_j is again given by 2.6. Thus, for $|\psi\rangle = |q\rangle$, it does not really matter whether the post-selection occurs before or after the final projection.

The situation is more interesting if the measuring device is initialized as a superposition of different $|q\rangle$ states. In fact, in a realistic measurement process, preparing a definite eigenstate of $\hat{Q}$ might be difficult and the latter is more likely. We shall now examine what happens when the measuring device is initialized as such a superposition. As a specific example, we consider the case when the initial probe state is a Gaussian wave packet, i.e.,

$$\langle q|\psi_{\text{in}}\rangle = \frac{1}{(2\pi\sigma^2)^{1/4}}e^{-\frac{q^2}{4\sigma^2}} \tag{2.9}$$

The final probe wavefunction in q-space is given by (up to a normalization),

$$\begin{aligned}
\psi_{\text{fi}}(q) &= \langle\chi_{\text{fi}}|e^{-i\int \hat{H}(t)dt}|\psi_{\text{in}}\rangle|\chi_{\text{in}}\rangle \\
&= \langle\chi_{\text{fi}}|e^{-ig\hat{A}\hat{P}}|\psi_{\text{in}}\rangle|\chi_{\text{in}}\rangle \\
&= \langle\chi_{\text{fi}}|\sum_j\langle a_j|\chi_{\text{in}}\rangle\int dq e^{-g\hat{A}\frac{\partial}{\partial q}}e^{-\frac{q^2}{4\sigma^2}}|a_j\rangle|q\rangle \\
&= \sum_j\langle\chi_{\text{fi}}|a_j\rangle\langle a_j|\chi_{\text{in}}\rangle e^{-\frac{\left(q-ga_j\right)^2}{4\sigma^2}} \tag{2.10}
\end{aligned}$$

where we have used $\hat{H}(t) = \hat{H}_{int} = g(t)\hat{A}\hat{P}$ and hence, $\int dt\hat{H}(t) = g\hat{A}\hat{P}$ from the previous section. Note that the post-selection will not always be

successful. The probability of post-selection can be calculated as

$$P_r = \langle \psi_{\text{fi}} | \psi_{\text{fi}} \rangle = \langle \psi_{\text{in}} | \langle \chi_{\text{in}} | e^{ig\hat{A}\hat{P}} | \chi_{\text{fi}} \rangle \langle \chi_{\text{fi}} | e^{-ig\hat{A}\hat{P}} | \chi_{\text{in}} \rangle | \psi_{\text{in}} \rangle \qquad (2.11)$$

2.2.1 Post-selected measurements on spin-$\frac{1}{2}$ particles

We shall perform a post-selected measurement of spin with a von Neumann measuring device on spin-$\frac{1}{2}$ particles, where the measuring device is initialized as a Gaussian wave-packet. The analysis in this section closely follows the treatment by Duck *et al.* [21].

The experimental implementation requires a sequence of three Stern-Gerlach apparatus. We pass a beam of spin-$\frac{1}{2}$ particles, moving along the y-direction through an SG apparatus oriented such that the magnetic field makes an angle θ with the z-axis. The beam of particles splits into two beams, of which we select the one which is displaced upwards. This is our *pre-selection* step. By performing a projective measurement of $\hat{\sigma}_\theta$, and selecting only the $+1$ eigenstate, we are preparing our system in the initial state,

$$|\chi_{\text{in}}\rangle = \frac{1}{\sqrt{2}} \left(\left(\cos\frac{\alpha}{2} + \sin\frac{\alpha}{2} \right) |\uparrow\rangle + \left(\cos\frac{\alpha}{2} - \sin\frac{\alpha}{2} \right) |\downarrow\rangle \right) \qquad (2.12)$$

where $|\uparrow\rangle$ and $|\downarrow\rangle$ are the ± 1 eigenstates of $\hat{\sigma}_z$ respectively.

We measure the spin along z-direction on this pre-selected beam by passing it through a second SG apparatus, oriented along z-direction. The Hamiltonian for the measurement interaction is

$$\hat{H} = g(t)\hat{\sigma}_z \hat{Z} \qquad (2.13)$$

coupling the $\hat{\sigma}_z$ observable (system) with the position $\hat{Z}$ (measuring device). Following the von Neumann model, the measurement outcomes will be read off from the shifts in $\hat{P}_z$.

The final step is the post-selection, implemented by measuring $\hat{\sigma}_x$ with the third SG apparatus and considering only those particles that give $+1$ outcome. Therefore,

$$|\chi_{\text{fi}}\rangle = \frac{1}{\sqrt{2}} (|\uparrow\rangle + |\downarrow\rangle) \qquad (2.14)$$

The initial state of the measuring device is a Gaussian in momentum space,

$$\langle p_z | \psi \rangle = \frac{1}{(2\pi\sigma^2)^{1/4}} \exp\left[\frac{-p_z^2}{4\sigma^2} \right] \qquad (2.15)$$

The entire momentum-space wavefunction of the device will have p_x, p_y dependence but this is not relevant to the discussion and shall therefore

13

be ignored.

Then, using (2.10), the final wavefunction of the device in momentum space is,

$$\phi(p) = \left(\cos\frac{\alpha}{2} + \sin\frac{\alpha}{2}\right)\exp\left[\frac{-(p_z - g)^2}{4\sigma^2}\right]$$

$$+ \left(\cos\frac{\alpha}{2} - \sin\frac{\alpha}{2}\right)\exp\left[\frac{-(p_z + g)^2}{4\sigma^2}\right] \tag{2.16}$$

which is a superposition of two Gaussians. The corresponding probability density function is given by

$$g(p_z) = |\phi(p)|^2 \tag{2.17}$$

As there are two possible eigenvalues of $\hat{\sigma}_z$, we expect the pointer distribution to be peaked around two distinct shifts. This is in fact what we see if we observe our measuring device, before performing the post-selection. Post-selection would in that case only change the probability of outcomes ± 1.

But if we post-select *prior* to observing the pointer, because of interference, the probability density shows interesting behaviour at certain values of the parameters g, σ, α. For ease of analysis, we rewrite (2.16) in terms of the dimensionless quantities $P = \frac{p_z}{2\sigma}$ and $s = \frac{g}{2\sigma}$ as,

$$f(P) = \left(\cos\frac{\alpha}{2} + \sin\frac{\alpha}{2}\right)\exp\left[-(P - s)^2\right] + \left(\cos\frac{\alpha}{2} - \sin\frac{\alpha}{2}\right)\exp\left[-(P + s)^2\right] \tag{2.18}$$

Let us now examine the behaviour of $f(P)$ at different ranges of the parameters s and α.

Firstly, for $\alpha = 0$, our pre- and post-selected states are identical and the final probability distribution of the pointer is as we would expect. For large values of s, the distribution is sharply peaked at $\pm s$ [Fig. 2.1]. As s is decreased to 1, the two Gaussians start to overlap [Fig. 2.2], finally merging to give a probability distribution with a single peak for $s = 0.5$ [Fig. 2.3]. The large s limit is what we would demand for an ideal measurement, so as to clearly distinguish between the two peaks. Note that as the wavefunction is symmetric, the average shift in p_z is 0.

On increasing α to $\frac{\pi}{8}$, we find that in the large s limit, the behaviour is as expected, with two peaks of unequal magnitude at $\pm s$ [Fig. 2.3]. As s is decreased to 1, two peaks are still distinguishable, but they are now located at $P = -0.872$ and $P = 0.983$, i.e., the peaks are effectively displaced

14
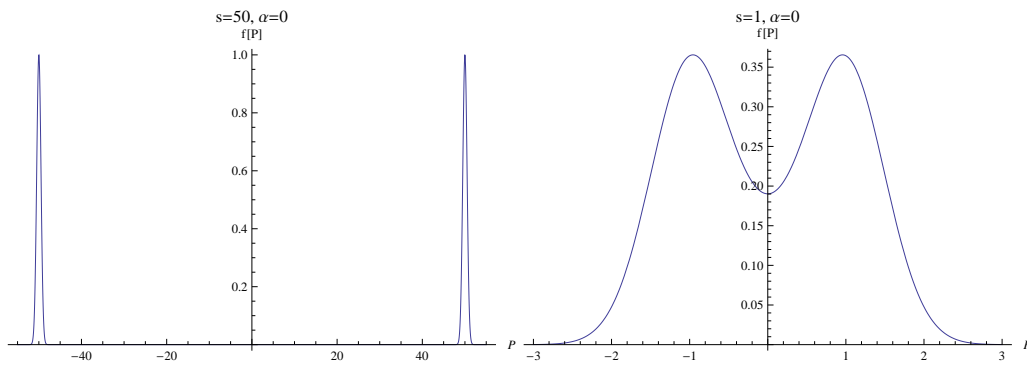
(a) $s = 50$. Graph shows two spikes at $P = \pm 50$

(b) $s = 1$. The two Gaussians interfere, but two peaks at ± 1 are still distinguishable.

Figure 2.1: Graph of $f(P)$ against P for $\alpha = 0$ and $s = 50, \ 1$.
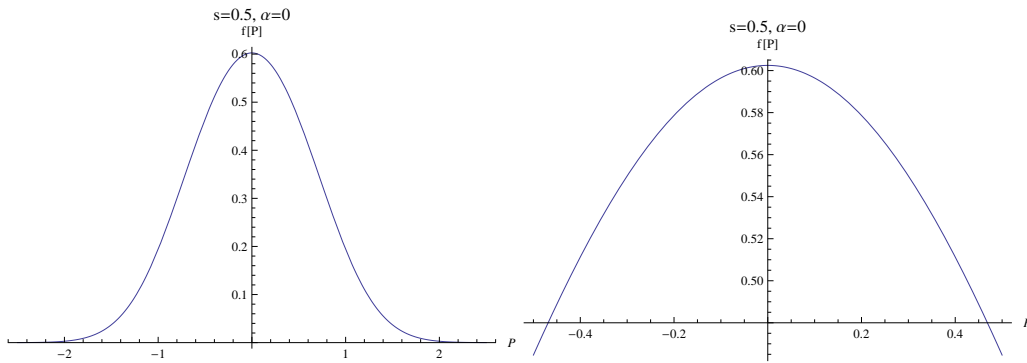
(a) Destructive interference produces a probability distribution with a single peak.

(b) A zoomed-in section of [c]. The function is peaked around 0.

Figure 2.2: Graph of $f(P)$ against P for $\alpha = 0$ and $s = 0.5$.

(a) $s = 2$. Two unequal peaks are clearly observed, located at ± 2.

(b) $s = 1$. The two Gaussians interfere and are barely distinguishable. The peaks here are located at $P = -1$ and $P = 0.973$

Figure 2.3: Graph of $f(P)$ against P for $\alpha = \frac{\pi}{8}$ and $s = 2,\ 1$.
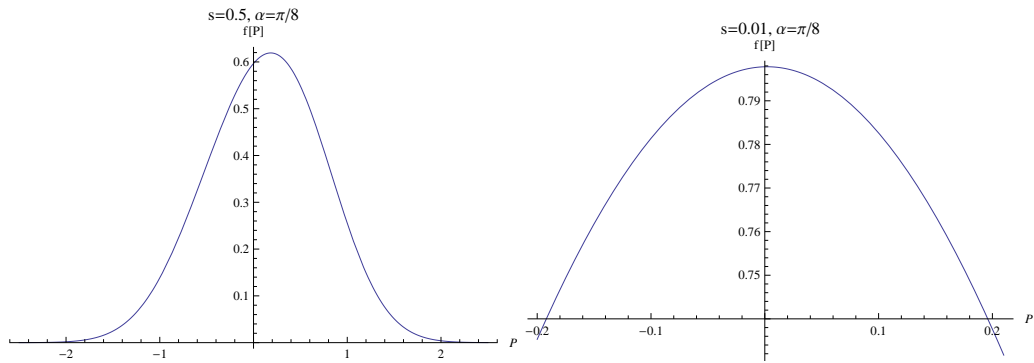
(a) Interference produces a probability distribution with a single peak at 0.184

(b) For $s = 0.01$ the function is peaked around $P = 0.002$.

Figure 2.4: Graph of $f(P)$ against P for $\alpha = \frac{\pi}{8}$ and $s = 0.5$.
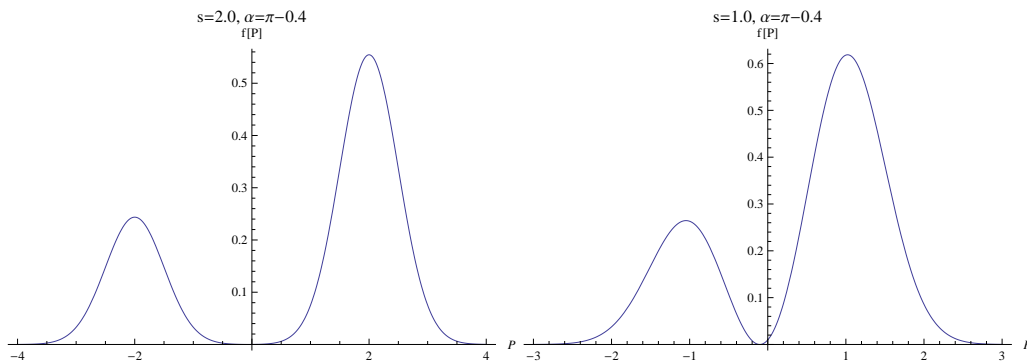
(a) $s = 2$. Two unequal peaks are clearly observed, located at ± 2.

(b) $s = 1$. The two Gaussians interfere and are barely distinguishable. The peaks here are located at $P = -1.047$ and $P = 1.022$.
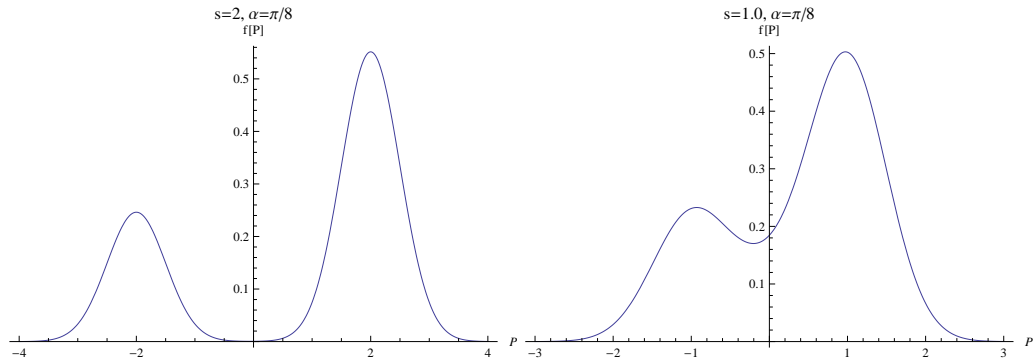
Figure 2.5: Graph of $f(P)$ against P for $\alpha = \pi - 0.4$ and $s = 2, \ 1$.
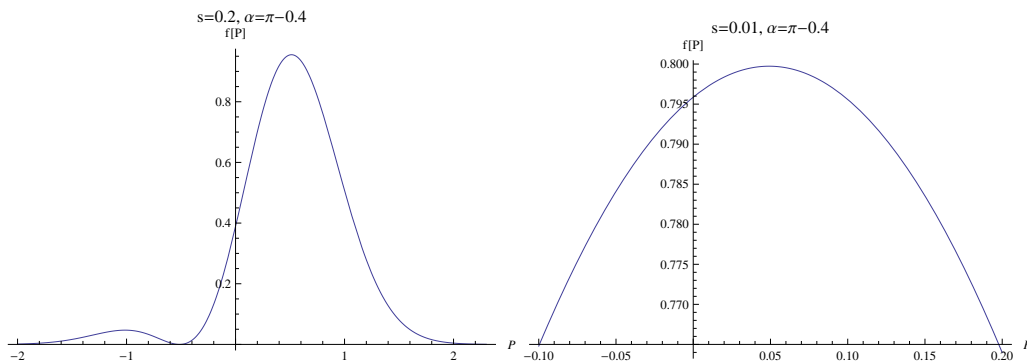
(a) Destructive interference produces a probability distribution with one large and one small peak for $s = 0.2$, located at $P = -1.014$ and $P = 0.514$ respectively.

(b) Final probability distribution is approximately a single Gaussian for $s = 0.01$, peaked around $P = 0.049$.

Figure 2.6: Graph of $f(P)$ against P for $\alpha = \pi - 0.4$ and $s = 0.5, \ 0.01$.

17

by an amount less than s. For $s = 0.5$, the two Gaussians merge to give approximately a single Gaussian, the peak being displaced through a distance $\delta P = 0.305$. $s = 0.01$ again gives a single Gaussian. The results are similar for $\alpha = \pi - 0.4$ [Fig. 2.5, Fig. 2.6].

We recall from chapter 2 that the measurement outcome is calculated as $\delta q/g$, i.e., $\delta p_z/g$ in this particular example. As the pointer states here are not eigenstates of $\hat{P}_z$, we can substitute in place of δp_z the displacements of the peaks of the probability distributions. While in several cases, the peaks are displaced by $\pm s$, thereby indicating outcomes ± 1, in many cases, the displacements are different from $\pm s$. A few such eccentric "measurement outcomes" m_z calculated in this manner are tabulated below: For $\alpha = \frac{\pi}{8}$,

α	s	P	$m_z = \delta P/s$
$\pi/8$	1	$0.973, -1$	$0.973, -1$
	0.5	0.184	0.368
$\pi - 0.4$	1	$1.022, -1.047$	$1.022, -1.047$
	0.2	$0.514, -1.014$	$2.57, -5.07$
	0.01	0.0491	4.91

Table 2.1: Pointer shifts and post-selected measurement outcomes

post-selected measurements yield outcomes which are less than or equal to 1. As we increase α, the measurement outcomes become larger than 1 in magnitude, as seen for $\alpha = \pi - 0.4$. For small values of s, we effectively have only one measurement outcome, which is many times larger than the largest eigenvalue of σ_z. In a way, this is puzzling, as classically post-selection is equivalent to choosing a particular sub-ensemble from a larger ensemble. From a probability distribution given by $|\chi_i\rangle$, we are selecting out a definite state $|\chi_f\rangle$ and asking what is the value of $\hat{\sigma}_z$ recorded by the measuring device for particles in this particular state. As there are only two possible values of the outcome, classically there is no way in which we can obtain such eccentric values. Quantum mechanically however, this is not that surprising, as our post-selected state has no well-defined value of spin along z-direction and is therefore not equivalent to a sub-ensemble. The measurement interaction entangles the system and the probe states, and in case of an ideal von Neumann measurement, establishes a one-to-one correspondence between the eigenvalues and pointer shifts. As we allow uncertainty in our pointer state, a clear one-to-one correspondence

is not established, which is why we see a single peak in the final pointer state for small s.

The limit of small s where the final distribution tends to a single Gaussian is the *weak measurement* limit mentioned previously. We discuss weak measurements and weak values more generally in the next section.

2.3 Weak measurements

As indicated in the previous section, weak measurements are a special case of measurements with post-selection. In this section, we show how weak values arise and introduce the general formalism for studying weak measurements. The starting point of our discussion on weak measurements is the final pointer state after post-selection,

$$|\psi_{\text{fi}}\rangle = \langle\chi_{\text{fi}}|e^{-ig\hat{A}\hat{P}}|\psi_{\text{in}}\rangle|\chi_{\text{in}}\rangle \tag{2.19}$$

Expanding in powers of g,

$$|\psi_{\text{fi}}\rangle = \langle\chi_{\text{fi}}|\left(I - ig\hat{A}\hat{P} + \cdots\right)|\psi_{\text{in}}\rangle|\chi_{\text{in}}\rangle$$
$$= \left(\langle\chi_{\text{fi}}|\chi_{\text{in}}\rangle - ig\langle\chi_{\text{fi}}|\hat{A}|\chi_{\text{in}}\rangle\hat{P} + \cdots\right)|\psi_{\text{in}}\rangle \tag{2.20}$$

If the coupling strength g is small, it is sufficient to retain terms up to first order,

$$|\psi_{\text{fi}}\rangle \approx \langle\chi_{\text{fi}}|\chi_{\text{in}}\rangle\left(I - ig\langle\hat{A}\rangle_{\text{w}}\hat{P}\right)|\psi_{\text{in}}\rangle \tag{2.21}$$

and re-sum to get the exponential back,

$$|\psi_{\text{fi}}\rangle \approx \langle\chi_{\text{fi}}|\chi_{\text{in}}\rangle e^{-ig\langle\hat{A}\rangle_{\text{w}}\hat{P}}|\psi_{\text{in}}\rangle \tag{2.22}$$

where we define $\langle\hat{A}\rangle_{\text{w}}$ as the *weak value* of $\hat{A}$, given by

$$\langle\hat{A}\rangle_{\text{w}} = \frac{\langle\chi_{\text{fi}}|\hat{A}|\chi_{\text{in}}\rangle}{\langle\chi_{\text{fi}}|\chi_{\text{in}}\rangle} \tag{2.23}$$

If our initial state is a Gaussian, using (2.9) in (2.22), we get

$$\psi(q) = e^{-\frac{(q-g\langle\hat{A}\rangle_{\text{w}})^2}{4\sigma^2}} \tag{2.24}$$

which is the displaced Gaussian we obtained for our post-selected measurement of spin in the previous section. The approximations used in this

19

calculation are, however, valid subject to several conditions. Firstly, the resummation performed to obtain (2.22) from (2.21) requires

$$|gp\langle\hat{A}\rangle_{\mathrm{w}}| \ll 1 \qquad (2.25)$$

Then, to neglect higher order terms in (2.20), we need

$$|g^n p^n \langle\chi_{\mathrm{fi}}|\hat{A}^n|\chi_{\mathrm{in}}\rangle| \ll |gp\langle\chi_{\mathrm{fi}}|\hat{A}|\chi_{\mathrm{in}}\rangle| \qquad (2.26)$$

Both (2.25) and (2.26) can be derived from an expansion of (2.20) in the $|p\rangle$ basis.

Now, note that for a Gaussian wave packet as in (2.9), the uncertainty in p, ΔP is of the order $1/\sigma$. Effectively, the wavefunction is localized within the limits $\pm\Delta p$, which allows us to replace p in (2.25) and (2.26) with $1/\sigma$, giving

$$\frac{\sigma}{g} \gg |\langle\hat{A}\rangle_{\mathrm{w}}| \qquad (2.27)$$

$$\frac{\sigma}{g} \gg \left|\frac{\langle\chi_{\mathrm{fi}}|\hat{A}^n|\chi_{\mathrm{in}}\rangle}{\langle\chi_{\mathrm{fi}}|\hat{A}|\chi_{\mathrm{in}}\rangle}\right|^{1/(n-1)} \quad \forall n \geq 2 \qquad (2.28)$$

If these conditions are satisfied, the final pointer state is approximately a single Gaussian displaced through the weak value. Therefore, the weak measurement outcome as recorded by the measuring device is the weak value $\langle\hat{A}\rangle_{\mathrm{w}}$. As expected, conditions (2.27) and (2.28) are similar to the limit of small $s = \frac{g}{2\sigma}$ for which we obtained the final probability distribution as a single Gaussian in [2.2.1].

2.3.1 Weak measurement of spin

We go back to our example of spin-$\frac{1}{2}$ particle on which we performed a post-selected measurement of $\hat{\sigma}_z$. For the PPS defined by equations (2.12) and (2.14), the weak value is

$$\langle\hat{A}\rangle_{\mathrm{w}} = \tan\frac{\alpha}{2} \qquad (2.29)$$

which means that our Gaussian has been shifted by an amount $\delta p_z = g\tan\frac{\alpha}{2}$ as a result of the weak measurement.

The conditions (2.27) and (2.28) reduce to

$$\frac{\sigma}{g} \gg \min\left[\tan\frac{\alpha}{2}, \cot\frac{\alpha}{2}\right] \qquad (2.30)$$

A large weak value, and hence a larger shift in the pointer, is observed when $|\tan\frac{\alpha}{2}|$ is greater than 1, i.e., $\alpha > \pi/4$. By letting $\alpha \to \pi$, the measurement outcome can be made arbitrarily large, provided we have, $\frac{\sigma}{g} \gg \cot\frac{\alpha}{2}$. Under these conditions, the two small shifts of $\pm g$ combine to give a large shift of $g\tan\frac{\alpha}{2}$. As noted by AAV in their original work [2], the weak measurement outcome can be as much as 100 times larger than the maximum eigenvalue.

2.3.2 Properties of weak values

Firstly the weak values depend on our choice of PPS and can accordingly be larger or smaller than the corresponding eigenvalues. For suitable choice of PPS, they can even be complex. In that case, only measuring shift in $\hat{Q}$ does not give us complete information about the weak value. Starting with a Gaussian pointer state, the final pointer wavefunction in q space is then,

$$\psi(q) \propto \exp\left[-\frac{(q - g\Re\langle\hat{A}\rangle_{\mathrm{w}} - ig\Im\langle\hat{A}\rangle_{\mathrm{w}})^2}{4\sigma^2}\right] \tag{2.31}$$

From this we obtain the following results:

$$\delta q = g\Re\langle\hat{A}\rangle_{\mathrm{w}}$$
$$\delta p = \frac{g}{2\sigma^2}\Im\langle\hat{A}\rangle_{\mathrm{w}} \tag{2.32}$$

i.e., the shift in the probe coordinate is now proportional to the real part of the weak value. The imaginary part of the weak value manifests itself as a shift in the momentum of the measuring device [22]. Also, it should be noted that even for a finite dimensional observable, the set of weak values is infinite.

Secondly, weak values are obtained in the limit $\sigma \gg g\langle\hat{A}\rangle_{\mathrm{w}}$, which implies that a single weak measurement has a very large associated uncertainty. Therefore, a statistically significant result is obtained only when the average weak value is computed over a large number of trials. This average approaches our theoretical weak value. Unlike an ideal projective measurement, a single ideal weak measurement is essentially of no use.

Also, as post-selection is not always successful, to obtain N successful weak measurement outcomes, NP such measurements are required, where P is the probability of successful post-selection. It is related to the overlap $|\langle\chi_{\mathrm{in}}|\chi_{\mathrm{fi}}\rangle|$ for general post-selected measurements and reduces to exactly that in the 1$^{\text{st}}$ approximation.

Unlike projective measurement outcomes, weak values display properties that one would expect from classical measurement. For instance, weak values are additive: the weak values of three operators related as $\hat{C} = \hat{A} + \hat{B}$, are also similarly related, $\langle \hat{C} \rangle_{\text{w}} = \langle \hat{A} \rangle_{\text{w}} + \langle \hat{B} \rangle_{\text{w}}$. This holds even if $\hat{A}$ and $\hat{B}$ do not commute. In that case, however, they cannot be measured jointly using standard projections and therefore such a relation cannot arise. For instance, we may take $\hat{A}$, $\hat{B}$ and $\hat{C}$ to be $\hat{\sigma}_x$, $\hat{\sigma}_y$ and $\frac{1}{\sqrt{2}}(\hat{\sigma}_x + \hat{\sigma}_y)$ respectively. These are operators for measuring spin along three different directions, the eigenvalues for all of them being ± 1. We cannot have a set of outcomes $\{a, b, c\}$ that will follow $c = a + b$. But for weak measurement outcomes, such additivity seems to hold, as one would expect for classical measurement outcomes. This allows weak values of non-commuting observables to form a consistent truth table.

2.3.3   Are weak measurements at all measurements?

Promoting weak values to the status of actual properties of a system on the basis of them obeying rules of classical logic is questionable, as this invites the problem of eccentric and even complex measurement outcomes.

Furthermore, von Neumann devised his model so that the changes in the measuring device had a one-to-one correspondence with the eigenvalues. As noted before, post-selection along with an uncertainty in initial pointer state destroys this correspondence. The subsequent definition of post-selected measurement outcome as the pointer shift divided by the coupling strength is therefore a departure from von Neumann's model and needs to be justified. Additionally, in the limit of the weak measurement, the measuring device fails to resolve the different eigenstates of an observable.

The weak values, and post-selected pointer shifts in general, do characterize the particular pre- and post-selection, but how it relates to the measurement of an observable continues to be debated.

2.4   General method for calculating average shifts

A single weak measurement has a large associated uncertainty, which is why average displacements of the pointer observables are more relevant than the displacements of the peaks. In this section we outline a general method for calculating average pointer shifts for general post-selected measurements, used previously Wu & Zukowski [23] and Puentes *et al.*

[24]. Weak-value induced shifts are obtained by taking the appropriate limit. These will be subsequently used in the Chapter 3 to calculate amplification factors.

Here, our measurement interaction is $\hat{H} = g(t)\hat{A}\hat{P}$ with $\int g(t)dt = g$, pre-selected and post-selected states are $|\chi_{\text{in}}\rangle$ and $|\chi_{\text{fi}}\rangle$ respectively, and initial pointer state $|\psi_{\text{in}}\rangle$. The pointer state after measurement interaction and post-selection is (up to a normalization)

$$|\psi_{\text{fi}}\rangle = \langle\chi_{\text{fi}}|e^{-ig\hat{A}\hat{P}}|\chi_{\text{in}}\rangle|\psi_{\text{in}}\rangle \tag{2.33}$$

The average shift in any observable $\hat{M}$ of the pointer is given by,

$$\langle\delta\hat{M}\rangle = \langle\hat{M}\rangle_{\text{fi}} - \langle\hat{M}\rangle_{\text{in}} \tag{2.34}$$

where

$$\langle\hat{M}\rangle_{\text{fi}} = \frac{\langle\psi_{\text{fi}}|\hat{M}|\psi_{\text{fi}}\rangle}{\langle\psi_{\text{fi}}|\psi_{\text{fi}}\rangle} \tag{2.35}$$

We can calculate these quantities by expanding $e^{-ig\hat{A}\hat{P}}$ is powers of g. Retaining terms up to 2$^{\text{nd}}$ order,

$$|\psi_{\text{fi}}\rangle = \langle\chi_{\text{fi}}|\chi_{\text{in}}\rangle(I - ig\langle\hat{A}\rangle_{\text{w}}\hat{P} - \frac{g^2}{2}\langle\hat{A}\rangle_{\text{w}}^2\hat{P}^2)|\psi_{\text{in}}\rangle \tag{2.36}$$

The probability of post-selection is

$$W = \langle\psi_{\text{fi}}|\psi_{\text{fi}}\rangle$$
$$= |\langle\chi_{\text{fi}}|\chi_{\text{in}}\rangle|^2 \left[I + 2g\Im\langle\hat{A}\rangle_{\text{w}}\langle\hat{P}\rangle_{\text{in}} + g^2(|\langle\hat{A}\rangle_{\text{w}}|^2 - \Re\langle\hat{A}^2\rangle_{\text{w}})\langle\hat{P}^2\rangle_{\text{in}}\right] \tag{2.37}$$

The term $\Im\langle\hat{A}\rangle_{\text{w}}\langle\hat{P}\rangle_{\text{in}}$ disappears if our initial device state is centred around $p = 0$, which is what we have taken previously.

The final expectation value of $\hat{M}$ up to second order is

$$\langle\hat{M}\rangle_{\text{fi}} = \frac{1}{W}|\langle\chi_{\text{fi}}|\chi_{\text{in}}\rangle|^2 \left[\langle\hat{M}\rangle_{\text{in}} + 2g\Im(\langle\hat{A}\rangle_{\text{w}}\langle\hat{M}\hat{P}\rangle_{\text{in}})\right.$$
$$\left. +g^2\left(|\langle\hat{A}\rangle_{\text{w}}|^2\langle\hat{P}\hat{M}\hat{P}\rangle_{\text{in}} - \Re(\langle\hat{A}^2\rangle_{\text{w}}\langle\hat{M}\hat{P}^2\rangle_{\text{in}})\right)\right] \tag{2.38}$$

For 1$^{\text{st}}$ order approximation

$$W = |\langle\chi_{\text{fi}}|\chi_{\text{in}}\rangle \tag{2.39}$$

$$\langle\hat{M}\rangle_{\text{fi}} = \langle\hat{M}\rangle_{\text{in}} + 2g\Im(\langle\hat{A}\rangle_{\text{w}}\langle\hat{M}\hat{P}\rangle_{\text{in}}) \tag{2.40}$$

The shift in $\hat{M}$ in this approximation is

$$\langle\delta\hat{M}\rangle = 2g\Im(\langle\hat{A}\rangle_{\mathrm{w}}\langle\hat{M}\hat{P}\rangle_{\mathrm{in}}) \tag{2.41}$$

Substituting $\hat{Q}$ and $\hat{P}$ in place of $\hat{M}$ in (2.41), we get the following shifts for the initial Gaussian pointer state given by (2.9),

$$\langle\delta\hat{Q}\rangle = g\Re\langle\hat{A}\rangle_{\mathrm{w}}$$
$$\langle\delta\hat{P}\rangle = \frac{g}{2\sigma^2}\Im\langle\hat{A}\rangle_{\mathrm{w}} \tag{2.42}$$

which are effectively identical to (2.32).

For observables of the type $\hat{A}^2 = I$, the average shifts can be calculated exactly. We can expand the unitary as

$$e^{-ig\hat{A}\hat{P}} = I\cos(g\hat{P}) - iA\sin(g\hat{P}) \tag{2.43}$$

The probability of post-selection can be computed as

$$W = |\langle\chi_f|\chi_i\rangle|^2 \left\langle \cos^2(g\hat{P}) + |\langle\hat{A}\rangle_w|^2 \sin^2(g\hat{P}) + \Im(\langle\hat{A}_w\rangle)\sin(2g\hat{P}) \right\rangle_{\mathrm{in}} \tag{2.44}$$

The final expectation value of $\hat{M}$ is given by

$$\langle\hat{M}\rangle_f = \frac{1}{Z}\Big\langle \cos(g\hat{P})M\cos(g\hat{P}) + |\langle\hat{A}\rangle_w|^2\sin(g\hat{P})\hat{M}\sin(g\hat{P})$$
$$+ i\langle\hat{A}\rangle_w\sin(g\hat{P})\hat{M}\cos(g\hat{P}) + i\langle\hat{A}\rangle_w\cos(g\hat{P})\hat{M}\sin(g\hat{P})\Big\rangle_{\mathrm{in}} \tag{2.45}$$

where

$$Z = \frac{W}{|\langle\chi_f|\chi_i\rangle|^2} \tag{2.46}$$

2.5 Experimental realization and applications

Duck *et al.* in their paper proposed an optical version of post-selected measurements, whose experimental implementation documented eccentric weak values as predicted by AAV [7]. Here, the state of polarization is treated as a two-level system with two orthogonal directions of linear polarization as a basis. The position degree of freedom of the photon acts as a the pointer and the weak measurement interaction takes place in birefringent plate which separates the two polarization components spatially. Since then, other experiments using, for instance, spin-orbit interaction [11] and interferometry [12] have independently confirmed the existence of weak values and demonstrated their applicability in detecting and amplifying small signals.

2.6 Summary

In this chapter, we have modified the notion of quantum measurements in succeeding steps. We started with the von Neumann model of projective quantum measurements where pointer shifts probabilistically yield eigenvalues as outcomes. Applying a post-selection on the system being measured, we demonstrated how the measurement outcomes, as recorded by the pointers start to differ from the eigenvalues. Finally, we introduced the limit of a weak measurement, where the pointer's uncertainty is so large that it fails to reveal the individual eigenvalue and records a single shift with a very large spread. This measurement outcome of an operator, if it may be called so, is not constrained to be, or even constrained in the range of, the eigenvalues. It can even be complex, in which case shifts in the pointer's coordinate and its conjugate momentum record the real and imaginary parts of the weak value respectively. Despite these strange features, weak values follow some rules that classical measurement outcomes are expected to follow and hence there is an ongoing debate on whether these can be taken as actual measurement outcomes and elements of reality.

The derivation of post-selected measurements and weak values is, however, mathematically consistent and indeed weak values have been documented experimentally. Weak measurements have also found immense applications as tools in various precision measurement and signal amplification schemes. Weak measurements have also been utilized for directly measuring the quantum wavefunction and quantum state tomography.

Chapter 3

Weak-value Amplification

Weak measurements have found extensive use as a technique for signal enhancement. These have been used to amplify a tiny spin Hall effect[11], for ultrasensitive measurements of beam deflection[12] as well as for precision frequency measurements[25]. The advantage of using weak measurements is that they can produce larger pointer shifts than that possible through standard projection while contributing negligibly to the noise in the process.

In a first order approximation for Gaussian pointer states, the pointer shifts δq and δp are of order g. The noise introduced in the process can be estimated through the corresponding standard deviations, Δq and Δp. It is seen from (2.41) that the 2nd order moments, $\langle \hat{Q}^2 \rangle$ and $\langle \hat{P}^2 \rangle$ do not have any corrections up to 1st order in g. The uncertainties Δq and Δp are thus unaffected in this approximation. Weak measurements therefore provide a means to improve the signal-to-noise ratio (SNR), which is defined as $\mathcal{R} = \frac{\delta q}{\Delta q}$.

At this point, the following objection may be raised: Given an interaction strength g, large pointer shifts are only obtained in the limit of very large Δq, which makes weak measurements imprecise to begin with. Therefore, surely an improved SNR can be easily obtained by merely performing standard von Neumann measurements using a probe with small Δq. How is then weak-value amplification at all useful?

The answer is that weak value amplification is useful only when the interaction concerned is so small that standard projective measurement induced shifts are below the noise inherent in the experimental apparatus. Post-selected measurements provide a means to increase shifts beyond the noise threshold, without adding to the noise significantly.

In this chapter, we study higher order corrections to the pointer shifts, SNR's and amplification factors for observables of the type $\hat{A}^2 = I$ by computing exact expressions of the first and second order moments of pointer observables $\hat{Q}$ and $\hat{P}$. We also investigate the possibility of increasing pointer shifts and improving SNR by using modified pointer states such as Hermite Gauss (HG) and Laguerre Gauss (LG) modes. Both HG and LG optical beams can be easily produced experimentally and therefore these results have direct relevance.

3.1 Exact calculations of pointer moments and SNR

We are interested in calculating exactly the pointer shifts and uncertainties for observables of the type $\hat{A}^2 = I$. We shall compare the maximum shifts achievable for three different initial states of the pointer. As before, our interaction Hamiltonian is of the form

$$\hat{H}_{int} = g(t)\hat{A} \otimes \hat{P} \tag{3.1}$$

where $\hat{A}$ and $\hat{P}$ are observables of the system and the pointer respectively. The pre- and post-selections are $|\chi_{\text{in}}\rangle$ and $|\chi_{\text{fi}}\rangle$ respectively. We use (2.45) and (2.46) from the previous chapter in our calculations. Z refers to the probability of post-selection divided by $|\langle\chi_{\text{in}}|\chi_{\text{fi}}\rangle|$ and $\langle\hat{M}\rangle_{\text{fi}}$ is the expectation of an observable $\hat{M}$ after post-selection.

We proceed to calculate the moments $\langle\hat{X}\rangle_{\text{fi}}$, $\langle\hat{P}\rangle_{\text{fi}}$, $\langle\hat{X}^2\rangle_{\text{fi}}$ and $\langle\hat{P}^2\rangle_{\text{fi}}$ with the following three different initial pointer states.

$$\text{(i) } \psi(x) \propto e^{-\frac{x^2}{4\sigma^2}}$$

$$\text{(ii) } \psi(x) \propto xe^{-\frac{x^2}{4\sigma^2}}$$

$$\text{(iii) } \psi(x,y) \propto (x+iy)e^{-\frac{x^2+y^2}{4\sigma^2}} \tag{3.2}$$

(i) is the Gaussian wave packet which we used in our calculations of post-selected measurements using Stern-Gerlach apparatus.

(ii) is the same Gaussian with an x up front. It is the simplest example of what are know as Hermite Gauss modes, whose general expression would be

$$H_n\left(\frac{x}{\sigma}\right)e^{-\frac{x^2}{4\sigma^2}}$$

(iii) is the simplest example of Laguerre Gauss mode with radial index zero, whose general expression is

$$\psi(x,y) \propto (x+i\text{Sgn}(l)y)^{|l|}e^{-\frac{x^2+y^2}{4\sigma^2}} \tag{3.3}$$

The motivation behind using these as pointer states is that these can be generated as optical beams and are therefore relevant to quantum optics implementations of weak-value amplification techniques.

For the remainder of this section, we shall drop the subscript "fi" and all expectation values will be assumed to have been calculated for the final pointer state after post-selection. Now, there are two different length scales here whose relative magnitudes essentially determine whether the measurement interaction is weak or not. These are g and σ, and it is convenient to express everything in terms of the dimensionless quantity $s = \frac{g^2}{2\sigma^2}$. For pointers initialized as Gaussians, we get the following results in terms of s and the weak values $\langle \hat{A} \rangle_{\mathrm{w}}$,

$$Z = \frac{1}{2} \left[1 + |\langle \hat{A} \rangle_{\mathrm{w}}|^2 + \left(1 - |\langle \hat{A} \rangle_{\mathrm{w}}|^2 \right) e^{-s} \right] \tag{3.4}$$

$$g\langle \hat{P} \rangle_f = \frac{\Im\langle \hat{A} \rangle_{\mathrm{w}} s e^{-s}}{Z} \tag{3.5}$$

$$\frac{\langle \hat{X} \rangle_f}{g} = \frac{\Re\langle \hat{A} \rangle_{\mathrm{w}}}{Z} \tag{3.6}$$

$$g^2 \langle \hat{P}^2 \rangle_w = \frac{s}{4Z} \left[\left(1 + |\langle \hat{A} \rangle_{\mathrm{w}}|^2 \right) + e^{-s} \left(|\langle \hat{A} \rangle_{\mathrm{w}}|^2 - 1 \right) (2s - 1) \right] \tag{3.7}$$

$$\frac{\langle \hat{X}^2 \rangle_w}{g^2} = \frac{1}{4sZ} \left[\left(1 - |\langle \hat{A} \rangle_{\mathrm{w}}|^2 \right) e^{-s} + \left(1 + |\langle \hat{A} \rangle_{\mathrm{w}}|^2 \right) (1 + 2s) \right] \tag{3.8}$$

The same quantities for the HG mode we have used are,

$$Z = \frac{1}{2} \left[1 + |\langle \hat{A} \rangle_{\mathrm{w}}|^2 + \left(1 - |\langle \hat{A} \rangle_{\mathrm{w}}|^2 \right) (1 - 2s) e^{-s} \right] \tag{3.9}$$

$$g\langle \hat{P} \rangle_f = \frac{\Im\langle \hat{A} \rangle_{\mathrm{w}}}{Z} s e^{-s} (2s - 3) \tag{3.10}$$

$$\frac{\langle \hat{X} \rangle_f}{g} = \frac{\Re\langle \hat{A} \rangle_{\mathrm{w}}}{Z} \tag{3.11}$$

$$g^2 \langle \hat{P}^2 \rangle_w = \frac{s}{4Z} \left[3 + 3|\langle \hat{A} \rangle_{\mathrm{w}}|^2 + \left(1 - |\langle \hat{A} \rangle_{\mathrm{w}}|^2 \right) e^{-s} (4s^2 - 12s + 3) \right] \tag{3.12}$$

$$\frac{\langle \hat{X}^2 \rangle_w}{g^2} = \frac{1}{4sZ} \left[\left(|\langle \hat{A} \rangle_{\mathrm{w}}|^2 - 1 \right) e^{-s} (2s - 3) + \left(1 + |\langle \hat{A} \rangle_{\mathrm{w}}|^2 \right) (2s + 3) \right] \tag{3.13}$$

Finally, for the LG mode we have,

$$Z = \frac{1}{2}\left[\left(1 + e^{-s}(1-s)\right) + |\langle\hat{A}\rangle_\text{w}|^2\left(1 + e^{-s}(s-1)\right)\right] \tag{3.14}$$

$$g\langle\hat{P}\rangle_f = -\frac{\Im(\langle\hat{A}\rangle_\text{w})}{Z}s(s-2)e^{-s} \tag{3.15}$$

$$\frac{\langle\hat{X}\rangle_f}{g} = \frac{\Re\langle\hat{A}\rangle_\text{w}}{Z} \tag{3.16}$$

$$g^2\langle\hat{P}^2\rangle_f = \frac{s}{2Z}\left[\left(1 + |\langle\hat{A}\rangle_\text{w}|^2\right) + e^{-s}\left(1 - |\langle\hat{A}\rangle_\text{w}|^2\right)\left(s^2 - \frac{7s}{2} + 1\right)\right] \tag{3.17}$$

$$\frac{\langle\hat{X}^2\rangle_f}{g^2} = \frac{1}{4Z}\left[2\left(1 + |\langle\hat{A}\rangle_\text{w}|^2\right)\left(1 + \frac{1}{s}\right) + e^{-s}\left(|\langle\hat{A}\rangle_\text{w}|^2 - 1\right)\left(1 - \frac{2}{s}\right)\right] \tag{3.18}$$

As can be seen, the factor Z is significantly changed in the exact calculation. This in turn also modifies the 1st order moments, $\langle\hat{X}\rangle$ and $\langle\hat{P}\rangle$. Note that $\langle\hat{X}\rangle$ is virtually unchanged in all cases expect for that due to the factor Z. The second order moments $\langle\hat{X}^2\rangle$ and $\langle\hat{P}^2\rangle$, which were unchanged up to 1st order in g are also noticeably changed.

3.1.1 Comparison of pointer shifts after post-selection

We estimate and compare the maximum shifts achieved using these three different pointer states. For this purpose, we choose the following pre- and post-selected states

$$|\chi_\text{in}\rangle = \frac{1}{\sqrt{2}}\left(\left(\cos\frac{\alpha}{2} + \sin\frac{\alpha}{2}\right)|\uparrow\rangle + \left(\cos\frac{\alpha}{2} - \sin\frac{\alpha}{2}\right)|\downarrow\rangle\right) \tag{3.19}$$

$$|\chi_\text{fi}\rangle = \frac{1}{\sqrt{2}}\left(|\uparrow\rangle + |\downarrow\rangle\right) \tag{3.20}$$

where $\alpha \in (0,\pi)$ To observe shifts in $\hat{X}$, which are due to the real part of the weak value, a weak measurement of $\hat{\sigma}_z$ is performed, giving,

$$\langle\hat{\sigma}_z\rangle_w = \tan\frac{\alpha}{2} \tag{3.21}$$

The weak value here is entirely pure and the consequent shift in $\hat{P}$ will be 0. For observing shifts in $\hat{P}$, a weak measurement of $\hat{\sigma}_x$ will be performed, which gives a purely imaginary weak value

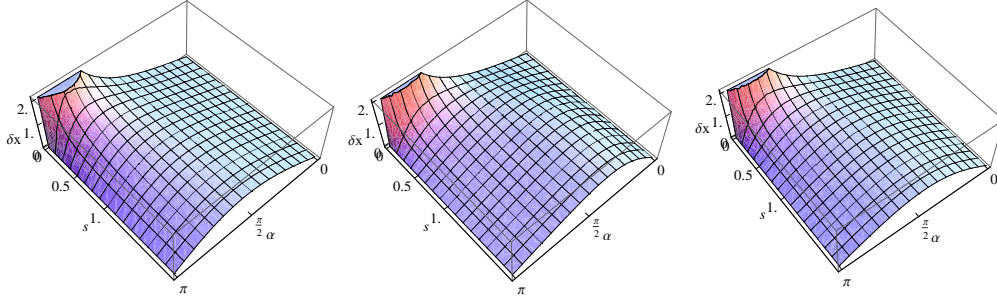$$\langle\hat{\sigma}_x\rangle_w = -i\tan\frac{\alpha}{2} \tag{3.22}$$

Figure 3.1: $\delta x = \frac{\langle \hat{X} \rangle}{g}$ as a function of the coupling parameter $s = \frac{g^2}{2\sigma^2}$ and the pre-selection angle α for pointers initialized as (a) Gaussian, (b) HG and (c) LG modes. For each value of s there exists an optimum pre-selection angle that maximizes δx.

Figure 3.2: $\delta p = g \langle \hat{P} \rangle$ as a function of the coupling parameter $s = \frac{g^2}{2\sigma^2}$ and the pre-selection angle α for pointers initialized as (a) Gaussian, (b) HG and (c) LG modes. For each value of s there exists an optimum pre-selection angle that maximizes δp.
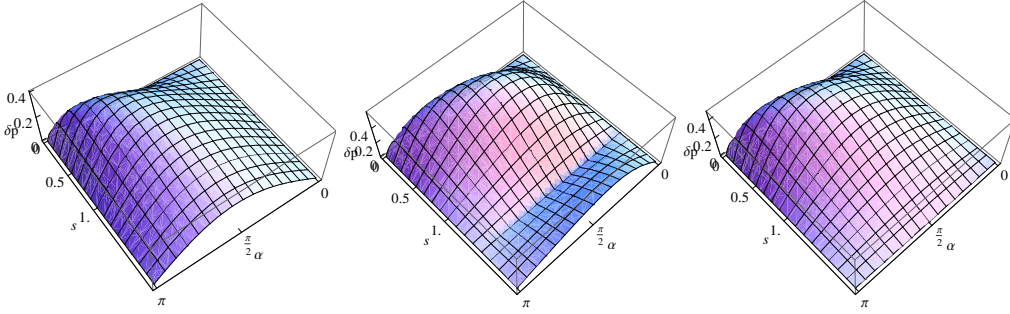
The pointer shifts in both $\hat{X}$ and $\hat{P}$ for the different initial pointer states in this scheme can be compared using the same parametrization of the weak value.

In all the figures, we have plotted scaled pointer shifts, viz. $\delta x = \frac{\langle \hat{X} \rangle}{g}$ and $\delta p = g \langle \hat{p} \rangle$. The 3D plots of Fig. 3.1 and Fig. 3.2 show that for each value of the coupling parameter s, an optimum value of α may be chosen, so as to maximize the pointer shift, either in x or in p. This has been previously indicated by Wu and Li, who calculated the pointer shifts up to second order in g[26], and also by Zhu *et al.*[27]. Maximum pointer shifts have also been calculated using exact expressions for Gaussian pointer states and $\hat{A}^2 = I$ type observables by Nakamura *et al.*[28]. Here, we have demonstrated similar results using alternate pointer states.
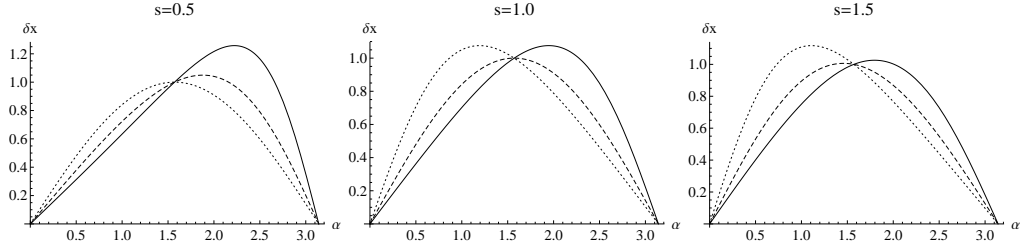
Figure 3.3: $\delta x = \frac{\langle \hat{X} \rangle}{g}$ as a function of the pre-selection angle α for different values of the coupling parameter $s = \frac{g^2}{2\sigma^2}$. Solid, dotted and dashed lines correspond to Gaussian, HG and LG modes respectively. For $s = 0.5$, Gaussian gives the maximum (over all possible α) shift, followed by LG and then HG. Gaussian and HG give comparable maximum shifts for $s = 1$, while LG gives a smaller shift. For $s = 1.5$, HG gives the largest possible shift, whereas the maximum shifts due to Gaussian and LG are smaller and almost equal.
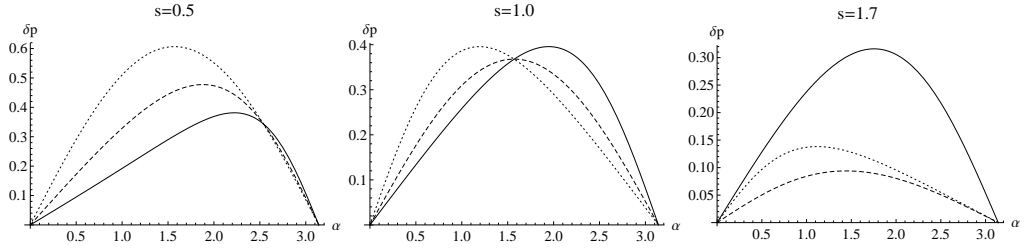
Figure 3.4: $\delta p = \frac{\langle \hat{P} \rangle}{g}$ as a function of the pre-selection angle α for different values of the coupling parameter $s = \frac{g^2}{2\sigma^2}$. Solid, dotted and dashed lines correspond to Gaussian, HG and LG modes respectively. For $s = 0.5$, HG gives the largest maximum shift, followed by LG and then Gaussian. For $s = 1$, the shifts produced by HG and Gaussian are equally large whereas LG gives a smaller shift. Gaussian gives the maximum possible shift for $s = 1.7$, with HG and LG giving successively smaller shifts.

Next, we compare the maximum shifts achievable for each of the three pointer states. With regard to maximum x-shifts, HG and LG both perform worse than the Gaussian pointer state for small values of s, i.e., in the limit of weak measurements, as seen from Fig. 3.3. The limit of s is the limit where the distinct eigenvalues are relatively well-resolved and therefore of relatively lesser interest. HG and LG give larger shifts than the Gaussian when s is increased. HG and LG perform better than a Gaussian initial state when s is small, but not as well when s is increased. In the limit where the weak measurement approximation holds, the HG and LG modes help in achieving larger shifts only in the momentum observable.

3.1.2   Comparison of signal-to-noise ratios

We now use the exact expressions for the various pointer moments to calculate the signal-to-noise ratio (SNR) for the three different initial states. For a single measurement, with a shift (which is the signal) δq and an associated uncertainty (noise) Δq, the signal-to-noise ratio is defined as

$$\mathcal{R} = \frac{\delta q}{\Delta q} \tag{3.23}$$

For N repeated standard projective measurements, the signal will be replaced by the expectation of an observable $\hat{Q}$, and the noise will be reduced by a factor $\sqrt{N}$,

$$\mathcal{R}_p = \sqrt{N} \frac{\langle \hat{Q} \rangle}{\Delta q} \tag{3.24}$$

In the case of the von Neumann model, $\langle \hat{Q} \rangle = g\langle \hat{A} \rangle$, where $\hat{A}$ is the observable being measured and $\hat{Q}$ is the pointer observable that records it. So

$$\mathcal{R}_p = \sqrt{N} \frac{g\langle \hat{A} \rangle}{\Delta q} \tag{3.25}$$

For post-selected measurements, both the numerator and denominator will be changed. In the specific case of weak measurements, where a 1$^{\text{st}}$ order approximation is sufficient, the uncertainty is unchanged and the average shift in $\hat{Q}$ is $g\Re\langle \hat{A} \rangle_{\text{w}}$. However, the number of successful trials in the post-selected case is reduced to NP, where P is the probability of post-selection and N is the total number of trials performed. The SNR in $\hat{Q}$ for a general post-selected measurement is

$$\mathcal{R}_w^{(q)} = \sqrt{NP} \frac{\langle \hat{Q} \rangle}{\sqrt{\langle \hat{Q}^2 \rangle - \langle \hat{Q} \rangle^2}} \tag{3.26}$$

In the 1st order approximation using Gaussian pointer states, the pointer shifts in x and p are

$$\delta x = g\Re\langle\hat{A}\rangle_{\mathrm{w}}$$

$$\delta p = \frac{g^2}{2\sigma^2}\Im\langle\hat{A}\rangle_{\mathrm{w}} \tag{3.27}$$

while the uncertainties are

$$\Delta q = \sigma$$

$$\Delta p = \frac{1}{2\sigma}$$

Therefore, to first order the SNR's are ,

$$\mathcal{R}_w^{(x)} = \sqrt{N}|\langle\chi_{\mathrm{in}}|\chi_{\mathrm{fi}}\rangle|\frac{g\Re\langle\hat{A}\rangle_{\mathrm{w}}}{\sigma} \tag{3.28}$$

$$\mathcal{R}_w^{(p)} = \sqrt{N}|\langle\chi_{\mathrm{in}}|\chi_{\mathrm{fi}}\rangle|\frac{g\Im\langle\hat{A}\rangle_{\mathrm{w}}}{\sigma} \tag{3.29}$$

The amplification factor over projective measurements are

$$\mathcal{K}_x = |\langle\chi_{\mathrm{in}}|\chi_{\mathrm{fi}}\rangle|\frac{\Re\langle\hat{A}\rangle_{\mathrm{w}}}{\langle\hat{A}\rangle} \tag{3.30}$$

As both $\Re\langle\hat{A}\rangle_{\mathrm{w}}$ and $\Im\langle\hat{A}\rangle_{\mathrm{w}}$ can be increased indefinitely by choice of pre- and post-selection, it appears from the first order expressions that the SNR's can be increased indefinitely. But quite obviously, this is not true. As seen in the previous section from exact expressions, the pointer shifts have an upper bound. Moreover, the uncertainties also increase due to higher order corrections. Consequently, there is a maximum value of the SNR that can be achieved using post-selection. We compare the maximum enhancement of SNR achieved for the three different pointer states using exact expressions. This can be calculated as,

$$\frac{\mathcal{R}_w^{(q)}}{\sqrt{N}} = |\langle\chi_{\mathrm{in}}|\chi_{\mathrm{fi}}\rangle|\frac{\langle\hat{Q}\rangle}{\sqrt{\langle\hat{Q}^2\rangle - \langle\hat{Q}\rangle^2}} \tag{3.31}$$

in which all the expectation values are to be calculated in the final pointer state.

From Figs. 3.5 and 3.6, it is clearly seen that the enhancement in SNR using post-selection has an upper limit. There exists an optimum angle of
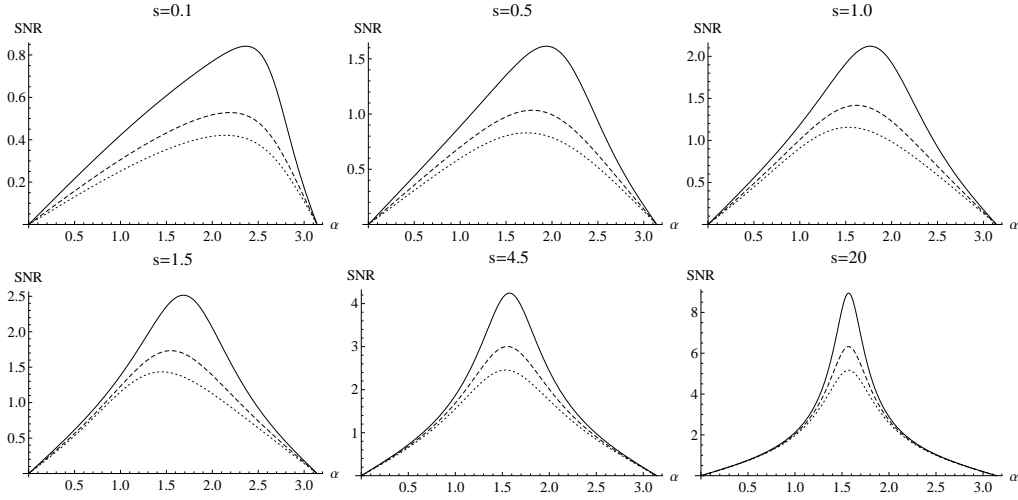
Figure 3.5: Representative plots of the SNR using x, $\mathcal{R}_w^{(x)}/\sqrt{N}$, plotted against α for $s = 0.1,\ 0.5,\ 1.0,\ 1.5,\ 4.5,\ 20$. Solid, dotted and dashed lines correspond to Gaussian, HG and LG modes respectively. The SNR for each has a maximum for at certain optimum values of α. Initially, for small s, the optimum angle shows s dependence but approaches $\pi/2$ for large s. Gaussian gives better SNR than HG and LG for all values of s.

pre-selection, which maximizes the SNR. The value of this optimum angle depends on the strength of the coupling, which here is given by s.

It is seen in Fig. 3.5 that the Gaussian wave packet as the initial pointer state gives the maximum possible SNR enhancement for pointer shifts in the x-variable. Using the alternate wavefunctions as initial states do not give any further enhancement. However, for shifts in the p-variable, use of LG and HG modes can in some cases give better SNR than the Gaussian. The alternate states give higher maximum SNR only in certain ranges of the coupling parameter s, the exact dependence on which is not clearly evident. Nevertheless, we have shown that exact calculations of the SNR yield an upper limit to signal enhancement. Furthermore, we have demonstrated that use of alternate wavefunctions as pointer initial states can produce further signal enhancement through observation of shifts in the pointer momentum.

3.2 Summary

In this chapter, we have studied the possibility of signal amplification through weak measurements. It has been shown how weak value in-
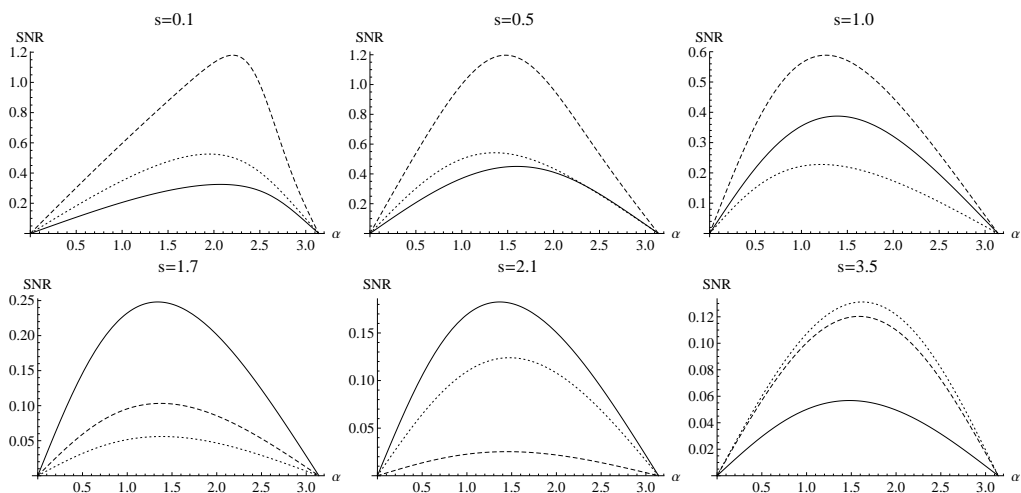
Figure 3.6: Representative plots of the SNR using p, $\mathcal{R}_w^{(p)}/\sqrt{N}$, plotted against α for $s = 0.1, \ 0.5, \ 1.0, \ 1.7, \ 2.1, \ 3.5$. Solid, dotted and dashed lines correspond to Gaussian, HG and LG modes respectively. The SNR for each has a maximum for at certain optimum values of α, which again depends on the value of s. For $s - 0.1, \ 0.5$, LG gives the maximum possible SNR, followed by HG and then Gaussian. When $s = 1$, LG still gives the highest, but Gaussian does better than HG. For $s = 1.7, \ 2.1$, Gaussian performs better than either. For $s = 3.5$ again, Gaussian performs worse than the other two.

duced large pointer shifts can be used to amplify and enhance the quality of small signals, as measured by the signal-to-noise ratio (SNR). Through exact calculations for idempotent observables, we have demonstrated that there is an upper limit to both maximum possible pointer shifts and SNR enhancement for post-selected measurements. We have also shown that by using alternate initial pointer distributions, such as simplified HG and LG modes, we can produce larger pointer shifts than that produced by Gaussian states. Likewise, the SNR of amplification, when measured for the p-variable shows an improvement in certain cases when such alternate pointer distributions are used.

Chapter 4

State Reconstruction with Post-selected Measurements

Weak measurements and more generally post-selected measurements have so far been defined according to a known pre- and post-selected ensemble. While weak measurement is a method of assigning a value to an observables consistent with the pre- and post-selection, it ought to be noted that if we already know the pre-selection, we know the projective measurement statistics of any observable on this system. We already know everything we can possibly determine by performing any quantum operation, including weak measurements. In the case of weak-value amplification, "system" and "pointer" are merely names and the essential process is that of amplifying and detecting an interaction using appropriate PPS and initial pointer states.

Now we ask the question, can post-selected measurements reveal anything about an unknown initial state of the system?

To answer this, we note that the average shifts of the pointer variable induced by a post-selection reveal some information about our pre-selected state, whether in the weak limit or beyond. It stands to reason therefore that post-selection induced pointer shifts can be used to determine various properties of an unknown quantum system. We can even infer the initial quantum state from the average shifts. Here, we illustrate this in the case of a spin-1/2 particle. The procedure is, however, fairly general and can be easily extended to more general systems. Weak measurements have been used in [16] to reconstruct a wavefunction. Also, methods quantum state tomography using weak measurements have been suggested by Hoffman [17] and Wu [29].

4.1 Reconstruction of a spin-$\frac{1}{2}$ state

In the typical post-selected measurement, we look at the shifts of the probe observable(s) after a post-selection, achieved through projective measurement of some operator, after which we chose to look at only one particular outcome of the final projection. However, nothing is stopping us from looking at all the possible outcomes of the final projection. That in fact, reveals information about the initial state of the system. Here we study this for a spin-$\frac{1}{2}$ system.

4.1.1 Pure state reconstruction

Suppose that we are given an unknown initial state (pre-selection) of this system,

$$|\chi_i\rangle = \cos\theta|\uparrow\rangle + e^{i\phi}\sin\theta|\downarrow\rangle \tag{4.1}$$

where $0 \leq \theta \leq \frac{\pi}{2}$ and $0 \leq \phi \leq 2\pi$. We perform a weak measurement of $\hat{\sigma}_z$, i.e., spin along z-direction, followed by a projection to the $|\pm\rangle$ basis, where $|\pm\rangle = \frac{1}{\sqrt{2}}(|\uparrow\rangle \pm |\downarrow\rangle)$. This implies that we finally perform a projective measurement of $\hat{\sigma}_x$ and observe the pointer shifts separately for each of the two outcomes. In other words, we determine the average pointer shifts for the $|+\rangle$ and $|-\rangle$ post-selection separately.

We recall that, given an interaction Hamiltonian of the form $g\delta(t)\hat{A} \otimes \hat{P}$, and the initial probe state as a Gaussian with $\Delta q = \sigma$ the average shifts in our probe observables, $\hat{Q}$ and $\hat{P}$ are, up to first order,

$$\delta q = g\Re\langle\hat{\sigma}_z\rangle_w \tag{4.2}$$

$$\delta p = \frac{g}{2\sigma^2}\Im\langle\hat{\sigma}_z\rangle_w \tag{4.3}$$

The weak values of $\hat{\sigma}_z$ for the $|\pm\rangle$ post-selections are respectively,

$$z_w^+ = \frac{\cos 2\theta - i\sin\phi\sin 2\theta}{1 + \cos\phi\sin 2\theta} \tag{4.4}$$

$$z_w^- = \frac{\cos 2\theta + i\sin\phi\sin 2\theta}{1 - \cos\phi\sin 2\theta} \tag{4.5}$$

where $z_w^\pm$ refers to the weak value of $\hat{\sigma}_z$ in the $|\pm\rangle$ post-selection respectively. By observing the average shifts in the pointer observables, we can determine the real and imaginary parts of the weak value for each post-selection. Now, as $\hat{Q}$ and $\hat{P}$ are canonical conjugates, at a time we can

determine shifts in only one of these two quantities. Therefore, we can access either the real part or the imaginary part of the weak value at a time. The real parts of the two weak values, as determined from the δq's are

$$\frac{\delta q_+}{g} = \frac{\cos 2\theta}{1 + \cos \phi \sin 2\theta} \tag{4.6}$$

$$\frac{\delta q_-}{g} = \frac{\cos 2\theta}{1 - \cos \phi \sin 2\theta} \tag{4.7}$$

The above two equations can be inverted to give,

$$\cos 2\theta = \frac{\delta q_+ \delta q_-}{g(\delta q_+ + \delta q_-)} \tag{4.8}$$

$$\cos \phi = \frac{1}{\sin 2\theta} \frac{\delta q_- - \delta q_+}{\delta q_- + \delta q_+} \tag{4.9}$$

Therefore, by calculating the average q-shifts in the pointer corresponding to each of the $|\pm\rangle$ eigenstates, we can calculate θ and ϕ. Likewise, average p-shifts can also be used for the same purpose.

The final projective measurement can be of the spin along any arbitrary direction instead of $\hat{\sigma}_x$, i.e, we can project on the basis

$$|\alpha_1\rangle = \cos \alpha |0\rangle + \sin \alpha |1\rangle$$
$$|\alpha_2\rangle = \sin \alpha |0\rangle - \cos \alpha |1\rangle \tag{4.10}$$

The q-shifts in the weak measurement limit for these two post-selections will be, respectively,

$$\frac{\delta q_1}{g} = \frac{\cos 2\theta + \cos 2\alpha}{1 + \cos 2\theta \cos 2\alpha + \cos \phi \sin 2\theta \sin 2\alpha} \tag{4.11}$$

$$\frac{\delta q_2}{g} = \frac{\cos 2\theta - \cos 2\alpha}{1 - \cos 2\theta \cos 2\alpha - \cos \phi \sin 2\theta \sin 2\alpha} \tag{4.12}$$

We can again solve for $\cos 2\theta$ and $\cos \phi$ from these two equations and determine them in terms of the pointer shifts and α,

$$\cos 2\theta = \frac{2\delta q_1 \delta q_2}{g(\delta q_1 + \delta q_2)} - \cos 2\alpha \tag{4.13}$$

$$\cos \phi = \frac{\cot 2\alpha}{\sin 2\theta} \frac{g}{\delta q_1 + \delta q_2} + \frac{1}{\sin 2\theta \sin 2\alpha} \frac{\delta q_2 - \delta q_1}{\delta q_1 + \delta q_2} - \cot 2\theta \cot 2\alpha \tag{4.14}$$

The pointer shifts given in (4.2) and (4.3) and hence the subsequent estimates for θ and ϕ are valid only to first order in g, as we have noted

before. For exact calculations, we may refer to equations (3.4), (3.5) and (3.6) which for the $|\pm\rangle$ post-selection will give

$$\frac{\delta q}{g} = \frac{2\Re(z_w^\pm)}{1 + |(z_w^\pm)|^2 + (1 - |(z_w^\pm)|^2)\, e^{-s}} \tag{4.15}$$

$$g\delta p = \frac{2\Im(z_w^\pm)se^{-s}}{1 + |(z_w^\pm)|^2 + (1 - |(z_w^\pm)|^2)\, e^{-s}} \tag{4.16}$$

where $z_w^\pm$ are as defined in (4.4) and (4.5) and $s = \frac{g^2}{2\sigma^2}$. From these, we get

$$|z_w^\pm|^2 = \frac{\cos^2 2\theta + \sin^2\phi\sin^2 2\theta}{1 + \cos^2\phi\sin^2 2\theta \pm 2\cos\phi\sin 2\theta} = \frac{1 \mp \cos\phi\sin 2\theta}{1 \pm \cos\phi\sin 2\theta} \tag{4.17}$$

$$\therefore 1 + |(z_w^\pm)|^2 + \left(1 - |(z_w^\pm)|^2\right)e^{-s} = \frac{2(1 \pm \cos\phi\sin 2\theta e^{-s})}{1 \pm \cos\phi\sin 2\theta} \tag{4.18}$$

Substituting the above and $\Re(z_w^\pm)$ in (4.15), we get

$$\frac{\delta q_+}{g} = \frac{\cos 2\theta}{1 + \cos\phi\sin 2\theta e^{-s}} \tag{4.19}$$

$$\frac{\delta q_-}{g} = \frac{\cos 2\theta}{1 - \cos\phi\sin 2\theta e^{-s}} \tag{4.20}$$

$$g\delta p_+ = \frac{se^{-s}\sin\phi\sin 2\theta}{1 + \cos\phi\sin 2\theta e^{-s}} \tag{4.21}$$

$$g\delta p_- = \frac{se^{-s}\sin\phi\sin 2\theta}{1 - \cos\phi\sin 2\theta e^{-s}} \tag{4.22}$$

which can again be inverted to give,

$$\cos 2\theta = \frac{\delta q_+ \delta q_-}{g(\delta q_+ + \delta q_-)} \tag{4.23}$$

$$\cos\phi = \frac{1}{e^{-s}\sin 2\theta}\frac{\delta q_- - \delta q_+}{\delta q_- + \delta q_+} \tag{4.24}$$

These two shifts allow us to completely characterize the initial state of the system, both in the weak measurement limit and exactly.

4.1.2 Mixed state reconstruction

The most general mixed state for an ensemble of spin-$\frac{1}{2}$ particles can be parametrized as follows:
p fraction in the state $|\psi_1\rangle = \cos\theta|\uparrow\rangle + e^{i\phi}\sin\theta|\downarrow\rangle$ and

$(1 - p)$ fraction in the state $|\psi_2\rangle = \sin\theta|\uparrow\rangle - e^{i\phi}\cos\theta|\downarrow\rangle$.
The corresponding density matrix is

$$\rho = \begin{pmatrix} \sin^2\theta + p\cos 2\theta & -\sin\phi\sin 2\theta \\ \sin\phi\sin 2\theta & \cos^2\theta - p\cos 2\theta \end{pmatrix} \tag{4.25}$$

When the final projection is on the $|\pm\rangle$ basis, the average pointer shifts are

$$\frac{\delta q_+}{g} = (\cos 2\theta)\frac{2p - c - 1}{1 - c^2} \tag{4.26}$$

$$\frac{\delta q_-}{g} = (\cos 2\theta)\frac{2p + c - 1}{1 - c^2} \tag{4.27}$$

$$g\delta p_+ = (se^{-s}\sin\phi\sin 2\theta)\frac{2p + c - 1}{1 - c^2} \tag{4.28}$$

$$g\delta p_- = (se^{-s}\sin\phi\sin 2\theta)\frac{2p - c - 1}{1 - c^2} \tag{4.29}$$

$$\tag{4.30}$$

where

$$c = e^{-s}\cos\phi\sin 2\theta \tag{4.31}$$

As there are four equations and three parameters to be determined, we can solve for θ and ϕ once we know all four average shifts. But here we run into a problem, as shifts in both q and p cannot be determined simultaneously. A possibly method to circumvent this would be to measure shifts in q for half the systems in the ensembles and shifts in p for the other half.

We once again outline the general procedure we have followed:

1. Given an unknown spin-state, perform an interaction of spin along any direction $\vec{n}$, $\hat{sigma} \cdot \vec{n}$ with the pointer, which is initiated as a Gaussian in position basis.

2. Perform projective measurement of spin along a different direction $\vec{m}$ and observe the pointer shifts corresponding to each projection.

3. Reconstruct initial state from the average shifts.

This is slightly different from the usual process of state tomography where one measures average spin along three independent directions and computes the different elements of the density matrix from the three averages.

4.2 Summary

This chapter looked at post-selected measurements from the viewpoint of what they can tell us about the system on which we perform these measurements. With the spin-$\frac{1}{2}$ system as an example, we showed that post-selected measurements can be utilized to reconstruct unknown quantum states. For this purpose, it became necessary to look at more than one post-selection, i.e., we computed average shifts corresponding to both possible outcomes of the final projection. For reconstructing a pure state, observing the shifts in only one pointer variable proves sufficient. In the case of a mixed state however, observing both the position and momentum shifts of the pointer is necessary.

Chapter 5

Conclusion

In this thesis we have studied the theory of quantum measurements with post-selection, which in a specific limit reduces to the weak measurements introduced by Aharonov, Albert and Vaidman. These were introduced to answer the following question: what is the value of a quantum observable on a system which is measured to be in a particular state of a different observable at a later time, i.e., a system which is post-selected? As two quantum observables do not commute and therefore disturb the measurements of each other, Aharonov, Albert and Vaidman came up with the idea of a weak measurement - a process that minimally disturbs the state of a quantum system and ideally does not affect the outcome of a latter measurement. Formulated as a modification of von Neumann's model of a quantum measurement, a weak measurement requires three conditions - a) the measuring device, or pointer, is prepared in an initial state which has a large uncertainty, b) the interaction with the measuring device is so weak that it does not affect the system, and c) the measuring device is observed once the system is later detected in a particular state of another observable. It was found that in certain cases, a measurement so defined repeatedly gives a single measurement outcome, but with a very large uncertainty. These outcomes of weak measurements, called weak values, form a consistent pattern but their validity as actual measurement outcomes is undermined by the fact that they can lie outside the range of eigenvalues and can even be complex. Nevertheless weak measurements have aided in re-analysing conceptual problems and paradoxes in quantum mechanics.

In the second chapter, we reviewed the basic theory of the measurement process, starting with the von Neumann model of measurement. We introduced post-selection and studied its implications, demonstrating the

limit in which weak measurements are obtained. The strange properties of post-selected measurement outcomes were shown to be a consequence of interference between non-orthogonal pointer states, which can give rise to the pointer state being shifted through a greater value than otherwise possible. Subsequently, we re-derived the weak measurement limit analytically and outlined the properties of weak values. A general method for calculating pointer shifts after post-selected measurements was also provided for use in subsequent chapters.

While the physical meaning of weak values continues to be debated, the fact that post-selected measurements can produce large shifts in the pointer device has found extensive use in signal amplification. A number of weak measurement based precision measurement and signal detection techniques have been proposed in recent years. The third chapter discussed weak value amplification and examined the possibility of using alternate pointer states such as simplified Hermite Gauss and Laguerre Gauss modes, comparing their performances with the commonly used Gaussian state. To explore the limits of signal amplification, exact calculations were done for the class of idempotent observables in a two-level system. The results confirmed previous observations that there is a limit to signal amplification achievable through post-selection. Further, it was shown that further enhancement of signal quality, as measured by the signal-to-noise ratio, is possible in certain cases using alternate pointer distributions.

The last chapter dealt with the subject of state reconstruction using post-selection based techniques. Differing from the earlier description of post-selected measurements where the initial state is already known, the aim in this case was to use pointer shifts to determine the initial state. It was shown that a pure state of a spin-$\frac{1}{2}$ system can be determined from post-selected pointer shifts, using both approximate and exact results. A method for reconstructing mixed states was also proposed. As the method outlined is fairly general, it can be easily extended to higher-dimensional systems.

Whether weak measurements constitute elements of quantum reality and can be given physical meaning may continue to be debated. However, post-selection along with appropriately designed measurement interactions and initial pointer states provide new ways to controlling, tweaking and extracting information from a quantum system. Post-selected measurements are therefore likely to find wide applications as useful tools for quantum information processing.

References

[1] Y. Aharonov, D. Z. Albert, A. Casher, and L. Vaidman, "Surprising quantum effects," *Physics Letters A*, vol. 124, pp. 199 – 203, 1987.

[2] Y. Aharonov, D. Z. Albert, and L. Vaidman, "How the result of a measurement of a component of the spin of a spin- *1/2* particle can turn out to be 100," *Phys. Rev. Lett.*, vol. 60, pp. 1351–1354, Apr 1988.

[3] A. J. Leggett, "Comment on "how the result of a measurement of a component of the spin of a spin-(1/2 particle can turn out to be 100"," *Phys. Rev. Lett.*, vol. 62, pp. 2325–2325, May 1989.

[4] A. Peres, "Quantum measurements with postselection," *Phys. Rev. Lett.*, vol. 62, pp. 2326–2326, May 1989.

[5] Y. Aharonov and L. Vaidman, "Aharonov and vaidman reply," *Phys. Rev. Lett.*, vol. 62, pp. 2327–2327, May 1989.

[6] Y. Aharonov, S. Popescu, D. Rohrlich, and L. Vaidman, "Measurements, errors, and negative kinetic energy," *Phys. Rev. A*, vol. 48, p. 4084, Dec 1993.

[7] N. W. M. Ritchie, J. G. Story, and R. G. Hulet, "Realization of a measurement of a "weak value"," *Phys. Rev. Lett.*, vol. 66, pp. 1107–1110, Mar 1991.

[8] G. J. Pryde, J. L. O'Brien, A. G. White, T. C. Ralph, and H. M. Wiseman, "Measurement of quantum weak values of photon polarization," *Phys. Rev. Lett.*, vol. 94, p. 220405, Jun 2005.

[9] Y. Aharonov, A. Botero, S. Popescu, B. Reznik, and J. Tollaksen, "Revisiting hardy's paradox: counterfactual statements, real measurements, entanglement and weak values," *Physics Letters A*, vol. 301, no. 3-4, pp. 130 – 138, 2002.

[10] J. S. Lundeen and A. M. Steinberg, "Experimental joint weak measurement on a photon pair as a probe of hardy's paradox," *Phys. Rev. Lett.*, vol. 102, p. 020404, Jan 2009.

[11] O. Hosten and P. Kwiat, "Observation of the spin hall effect of light via weak measurements," *Science*, vol. 319, no. 5864, pp. 787–790, 2008.

[12] P. B. Dixon, D. J. Starling, A. N. Jordan, and J. C. Howell, "Ultrasensitive beam deflection measurement via interferometric weak value amplification," *Phys. Rev. Lett.*, vol. 102, p. 173601, Apr 2009.

[13] S. Kocsis, B. Braverman, S. Ravets, M. J. Stevens, R. P. Mirin, L. K. Shalm, and A. M. Steinberg, "Observing the average trajectories of single photons in a two-slit interferometer," *Science*, vol. 332, no. 6034, pp. 1170–1173, 2011.

[14] A. M. Steinberg, "Conditional probabilities in quantum theory and the tunneling-time controversy," *Phys. Rev. A*, vol. 52, pp. 32–42, Jul 1995.

[15] A. M. Steinberg, "How much time does a tunneling particle spend in the barrier region?," *Phys. Rev. Lett.*, vol. 74, pp. 2405–2409, Mar 1995.

[16] J. S. Lundeen, B. Sutherland, A. Patel, C. Stewart, and C. Bamber, "Direct measurement of the quantum wavefunction," *Nature*, vol. 474, p. 188. mult. p, Dec 2011.

[17] H. F. Hofmann, "Complete characterization of post-selected quantum statistics using weak measurement tomography," *Phys. Rev. A*, vol. 81, p. 012103, Jan 2010.

[18] A. K. Pan and P. K. Panigrahi, "Cat state, sub-planck structure and weak measurement," *unpublished*.

[19] J. von Neumann, *Mathematical Foundations of Quantum Mechanics*. Princeton University Press, 1936.

[20] Y. Aharonov and D. Rohrlich, *Quantum Paradoxes*. Wiley-VCH, 2005.

[21] I. M. Duck, P. M. Stevenson, and E. C. G. Sudarshan, "The sense in which a "weak measurement" of a spin-*1/2* particle's spin component yields a value 100," *Phys. Rev. D*, vol. 40, pp. 2112–2117, Sep 1989.

[22] R. Jozsa, "Complex weak values in quantum measurement," *Phys. Rev. A*, vol. 76, p. 044103, Oct 2007.

[23] S. Wu and M. Żukowski, "Feasible optical weak measurements of complementary observables via a single hamiltonian," *Phys. Rev. Lett.*, vol. 108, p. 080403, Feb 2012.

[24] G. Puentes, N. Hermosa, and J. P. Torres, "Weak measurements with orbital-angular-momentum pointer states," *Phys. Rev. Lett.*, vol. 109, p. 040401, Jul 2012.

[25] D. J. Starling, P. B. Dixon, A. N. Jordan, and J. C. Howell, "Precision frequency measurements with interferometric weak values," *Phys. Rev. A*, vol. 82, p. 063822, Dec 2010.

[26] S. Wu and Y. Li, "Weak measurements beyond the aharonov-albert-vaidman formalism," *Phys. Rev. A*, vol. 83, p. 052106, May 2011.

[27] X. Zhu, Y. Zhang, S. Pang, C. Qiao, Q. Liu, and S. Wu, "Quantum measurements with preselection and postselection," *Phys. Rev. A*, vol. 84, p. 052111, Nov 2011.

[28] K. Nakamura, A. Nishizawa, and M.-K. Fujimoto, "Evaluation of weak measurements to all orders," *Phys. Rev. A*, vol. 85, p. 012113, Jan 2012.

[29] S. Wu, "State tomography via weak measurements," *Sci. Rep.*, vol. 3, Feb 2013.